SANDIA REPORT

SAND2015-9358
Unlimited Release
Printed October 2015

NRT Rotor Structural/Aeroelastic Analysis for the Preliminary Design Review

Brandon L. Ennis, Joshua A. Paquette

Prepared by
Sandia National Laboratories
Albuquerque, New Mexico 87185 and Livermore, California 94550

Sandia National Laboratories is a multi-program laboratory managed and operated by Sandia Corporation, a wholly owned subsidiary of Lockheed Martin Corporation, for the U.S. Department of Energy's National Nuclear Security Administration under contract DE-AC04-94AL85000.

Sandia National Laboratories

Issued by Sandia National Laboratories, operated for the United States Department of Energy by Sandia Corporation.

Available to DOE and DOE contractors from
U.S. Department of Energy
Office of Scientific and Technical Information
P.O. Box 62
Oak Ridge, TN 37831

Telephone: (865) 576-8401
Facsimile: (865) 576-5728
E-Mail: reports@adonis.osti.gov
Online ordering: http://www.osti.gov/bridge

Available to the public from
U.S. Department of Commerce
National Technical Information Service
5285 Port Royal Rd
Springfield, VA 22161

Telephone: (800) 553-6847
Facsimile: (703) 605-6900
E-Mail: orders@ntis.fedworld.gov
Online ordering: http://www.ntis.gov/help/ordermethods.asp?loc=7-4-0#online

SAND2015-9358
Unlimited Release
Printed October 2015

NRT Rotor Structural/Aeroelastic Analysis for the Preliminary Design Review

Brandon L. Ennis, Joshua A. Paquette
Wind Energy Technologies Department
Sandia National Laboratories
P.O. Box 5800, MS1124
Albuquerque, NM 87185

Abstract

This document describes the initial structural design for the National Rotor Testbed blade as presented during the preliminary design review at Sandia National Laboratories on October 28-29, 2015. The document summarizes the structural and aeroelastic requirements placed on the NRT rotor for satisfactory deployment at the DOE/SNL SWiFT experimental facility to produce high-quality datasets for wind turbine model validation. The method and result of the NRT blade structural optimization is also presented within this report, along with analysis of its satisfaction of the design requirements.

Acknowledgment

This work was performed by Sandia National Laboratories' Wind Energy Technologies Department with funding from the Department of Energy Wind and Water Power Technologies Office.

Document Revisions

Date	Version	Description
26-Oct-2015	1.00	Initial release.

This page intentionally left blank.

Contents

List of Figures

List of Tables

Nomenclature

DOE Department of Energy

SNL Sandia National Laboratories

SWiFT Scaled Wind Farm Technology

OEM Original Equipment Manufacturer

NRT National Rotor Testbed

V_{avg} average wind speed

I_{ref} average reference turbulence intensity

TI turbulence intensity

DLC Design Load Case

V_{in} wind turbine power curve cut-in wind speed

V_{out} wind turbine power curve cut-out wind speed

NTM Normal Turbulence Model

ETM Extreme Turbulence Model

V_{hub} wind turbine hub-height wind speed

V_r wind turbine power curve rated wind speed

V_{50} 50-year extreme wind gust

V_1 1-year extreme wind gust

ECD Extreme Coherent gust with Direction change

EWS Extreme Wind Shear

EWS Extreme Wind speed Model

NuMAD Numerical Manufacturing And Design tool

FAST Fatigue, Aerodynamics, Structures and Turbulence aeroelastic wind turbine simulator

F_d design load

γ_F partial safety factor due to load calculation

F_k characteristic load

γ_d partial safety factor used for critical displacements

γ_m partial safety factor due to material properties

γ_n partial safety factor due to consequences of failure

α blade station angle of attack

β blade station airfoil non-deflected set angle

U_∞ freestream wind speed

Ω wind turbine rotational speed

r wind turbine span radial location

$V_{e,OP}$ blade station out of plane body velocity

$V_{e,IP}$ blade station in plane body velocity

a axial induction factor

a' tangential induction factor

TSR Tip Speed Ratio

AoA Angle of Attack

σ normal distribution standard deviation

θ_i blade station torsional deflection

l blade element length

GJ blade element rigidity

$T_{n,PitchAxis}$ net torsion around the blade pitch axis

$M_{p,n}$ blade element airfoil pitching moment

L blade element airfoil lift force

D blade element airfoil drag force

ϕ blade element relative freestream wind angle to the rotation plane

s blade element sweep distance

d_{IP} blade element in plane displacement

p blade element prebend distance

d_{OP} blade element out of plane displacement

This page intentionally left blank.

Introduction

The National Rotor Testbed (NRT) blade purpose is to support wind turbine and wind farm model validation efforts. The blade follows a design for analysis approach to meet the requirements of the future initial experimental campaign at SWiFT for model validation. Additionally, a primary objective of the blade design is to test functional scaling of a utility size wind turbine to produce a similar wake, as described by Kelley in the aerodynamic design report of the NRT rotor [2]. It follows then that this blade may deviate significantly from a standard structural blade design due to the different objectives. The first validation campaign goal is to reduce complexity to test fewer modeling assumptions, and structurally this means producing a "rigid" blade so aeroelastic effects can be ignored to a known uncertainty. Future experimental campaigns are considered to include aeroelastic effects which cannot be ignored on utility-size wind turbines.

The analysis that follows describes the requirements placed on the NRT blade and rotor system and the resulting blade design along with its satisfaction of these requirements. Requirements are described in full detail for the NRT rotor in another report [3], including the structural blade requirements restated within this report. The first requirements tested are the traditional requirements wind turbine blades are designed to meet from the governing wind turbine design standards to ensure blade survivability. Additional requirements are placed on the blade which are unique to the end goal of the NRT rotor to enable a high-quality validation dataset. These additional requirements exist to reduce experimental uncertainty and model complexity.

This page intentionally left blank.

Chapter 1

Standard Blade Requirements

The standard blade requirements are those described by *IEC 61400-1 Ed.3: Wind turbines - Part 1: Design Requirements* [1]. These standards are tested on the SNL/DOE SWiFT facility experimental wind farm site where the NRT rotors will be operated. The SWiFT turbines have a hub height of 32 m and the NRT rotor will have the SWiFT OEM turbine rotor diameter of 27 m so as to not affect the wind farm turbine spacing.

The IEC design standard is in reference to the turbine site's particular conditions with the site being designated by a numeric class (I-III) based on average wind speed at hub height, and a letter (A-C) based on the average turbulence intensity at 15 m/s. This classification is listed in Table 1.1.

Table 1.1. IEC Site Classification [1].

Wind Turbine Class	I	II	III
V_{Avg} (m/s)	10	8.5	7.5
A	$I_{ref@15\ m/s}$: 0.16		
B	$I_{ref@15\ m/s}$: 0.14		
C	$I_{ref@15\ m/s}$: 0.12		

The atmospheric conditions at the SWiFT site have been analyzed using two years of data from Texas Tech University's 200 m meteorological tower. The average wind speed at the SWiFT turbine hub height is 6.5 m/s, making it a class III. The average turbulence intensity (TI) is shown in Figure 1.1, compared with the IEC turbulence classification TI curves. The grey background dots are each 10 min averages from the data with the orange line showing the bin-average of this data. At 15 m/s the orange line is below the C-class of turbulence, so the C-class is used. The NRT rotor is then designed to be a class III-C machine.

1.1 Standard Requirements Description

The standard requirements placed on the NRT rotor which have been analyzed to ensure the design will be survivable and not damage the SWiFT turbines are as follows:

Meet IEC Design Load Case Requirements.

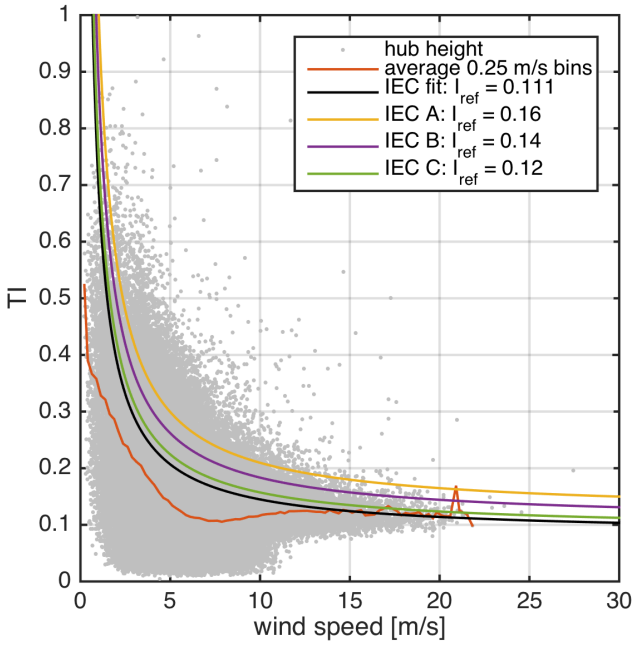

Figure 1.1. SWiFT Site IEC Turbulence Class.

Tip Deflection: Allowable tip deflection toward tower is 1.328 m, this includes total safety factor of 1.485.

Flap Frequencies: Flap frequencies not in the ranges of 2.9p-3.1p or 5.95p-6.05p.

Edge-Flap Frequency Ratio: The ratio of blade edgewise first natural frequency to flapwise first natural frequency shall be greater than 1.3.

Blade Mass: The manufactured blade mass shall be compared to the average weight of current OEM blades, 660 kg.

Rotor Inertia: The manufactured blade first moment of inertia shall be compared to the average moment of inertia of current OEM blade, 27,653 kg-m.

The IEC design load cases (DLC) analyzed in this initial structural design check are those which are most critical for the design and which are not testing a final turbine controller design. (It is noted that a final tuned controller would affect tip deflection during operation of the turbine, which will be checked in a detailed design of the blade.) The list of minimum design load cases to test as described by the standard is shown in Table 1.2, with the DLC's which are analyzed for the NRT rotor highlighted. The DLC's analyzed cover two categories of wind turbine operation with power production and a parked turbine with the rotor either locked or idling.

In the power production (Design Situation 1) load cases, 4 DLC's are analyzed. DLC 1.2 is a fatigue test resulting from atmospheric turbulence occurring from normal operation over the lifetime

of the machine. This load case is tested at wind speeds $[V_{in} : 2 : V_{out}]$ m/s using 6 random turbulence seeds to generate 10 min turbulent wind input files using the IEC normal turbulence model (NTM). DLC 1.3 is an ultimate strength test resulting from operation with extreme turbulence conditions. This load case is tested at wind speeds $[V_{in} : 2 : V_{out}]$ m/s using 6 random turbulence seeds to generate 10 min turbulent wind input files using the IEC extreme turbulence model (ETM). DLC 1.4 is an ultimate strength test resulting from operation near rated wind speed with an extreme coherent gust (15 m/s increase) with direction change ($720/V_{hub}$ deg) over a period of 10 sec. This load case is tested at $[V_r - 2, V_r, V_r + 2]$ m/s with both positive and negative direction change. DLC 1.5 is an ultimate strength test resulting from operation with a transient extreme wind shear event, both in the horizontal and vertical directions. The load case is tested at $[5 : 1 : 25]$ m/s for both positive and negative vertical wind shear.

In the extreme event, parked turbine (Design Situation 6) load cases, 2 DLC's are analyzed. DLC 6.1 is an ultimate strength test for a parked turbine with a 50-year wind gust event occurring along with yaw misalignment. This load case is tested at the V_{50} wind speed with discrete yaw misalignment of $[0, 5, 15]$ deg, positive and negative (for class III, the 50-year occurrence wind speed at hub height is 52.5 m/s). DLC 6.3 is an ultimate strength test for a parked turbine with a 1-year wind gust event occurring and yaw misalignment. This load case is tested at the V_1 m/s with yaw misalignment of $[0 : 5 : 30]$ deg, positive and negative (for class III, the 1-year occurrence wind speed at hub height is 30 m/s).

Table 1.2. IEC 61400-1 Minimum List of Design Load Cases [1].

Design situation	DLC	Wind condition		Other conditions	Type of analysis	Partial safety factors
1) Power production	1.1	NTM	$V_{in} < V_{hub} < V_{out}$	For extrapolation of extreme events	U	N
	1.2	NTM	$V_{in} < V_{hub} < V_{out}$		F	*
	1.3	ETM	$V_{in} < V_{hub} < V_{out}$		U	N
	1.4	ECD	$V_{hub} = V_r$-2 m/s, V_r, V_r+2 m/s		U	N
	1.5	EWS	$V_{in} < V_{hub} < V_{out}$		U	N
2) Power production plus occurrence of fault	2.1	NTM	$V_{in} < V_{hub} < V_{out}$	Control system fault or loss of electrical network	U	N
	2.2	NTM	$V_{in} < V_{hub} < V_{out}$	Protection system or preceding internal electrical fault	U	A
	2.3	EOG	$V_{hub} = V_r \pm 2$ m/s and V_{out}	External or internal electrical fault including loss of electrical network	U	A
	2.4	NTM	$V_{in} < V_{hub} < V_{out}$	Control, protection, or electrical system faults including loss of electrical network	F	*
3) Start up	3.1	NWP	$V_{in} < V_{hub} < V_{out}$		F	*
	3.2	EOG	$V_{hub} = V_{in}$, $V_r \pm$ 2m/s and V_{out}		U	N
	3.3	EDC	$V_{hub} = V_{in}$, $V_r \pm$ 2m/s and V_{out}		U	N
4) Normal shut down	4.1	NWP	$V_{in} < V_{hub} < V_{out}$		F	*
	4.2	EOG	$V_{hub} = V_r \pm 2$ m/s and V_{out}		U	N
5) Emergency shut down	5.1	NTM	$V_{hub} = V_r \pm 2$ m/s and V_{out}		U	N
6) Parked (standing still or idling)	6.1	EWM	50-year recurrence period		U	N
	6.2	EWM	50-year recurrence period	Loss of electrical network connection	U	A
	6.3	EWM	1-year recurrence period	Extreme yaw misalignment	U	N
	6.4	NTM	$V_{hub} < 0{,}7\ V_{ref}$		F	*
7) Parked and fault conditions	7.1	EWM	1-year recurrence period		U	A
8) Transport, assembly, maintenance and repair	8.1	NTM	V_{maint} to be stated by the manufacturer		U	T

Chapter 2

Structural Blade Optimization

The NRT blade structure is defined through a structural optimization process which varies the section component properties at the defined spanwise control stations to meet the optimization objective while constrained to satisfying the DLC's. The aerodynamic blade shape is fixed during the iterative structural optimization. The structural blade optimization is performed using NuMAD to manage the component structural changes with PreComp and BModes to estimate the blade structural properties. Design Load Cases are checked using the aeroelastic wind turbine simulator FAST, using the iteration's structural blade file from NuMAD. As part of the optimization, blade components are chosen to allow to vary both chordwise and spanwise with limits placed on that variation. Example component structural shell and a screenshot of the NuMAD GUI interface with the blade spanwise stations are shown in Figure 2.1.

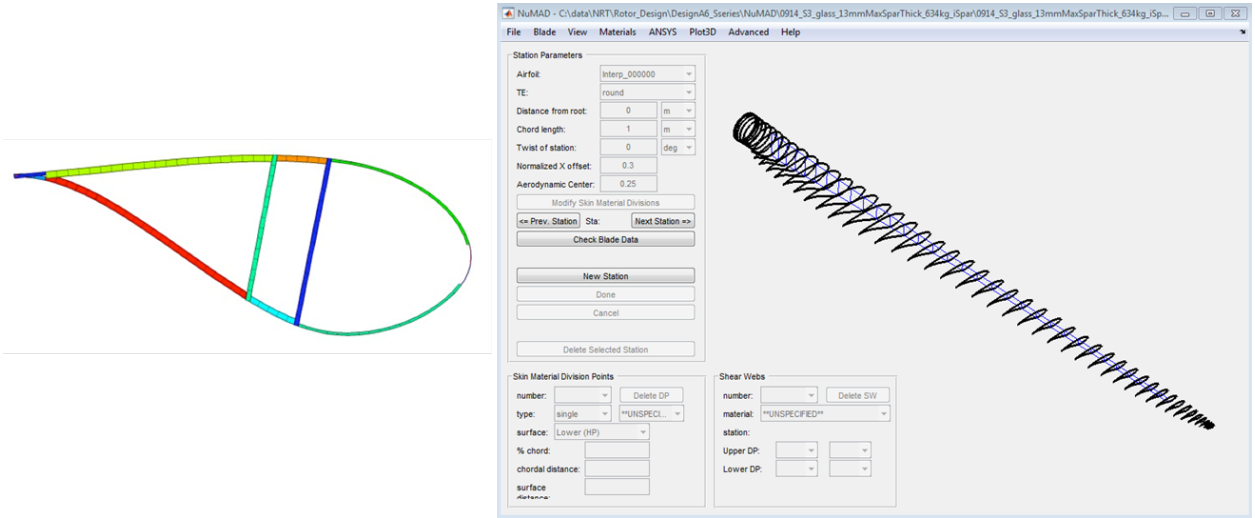

Figure 2.1. NuMAD Component Layup and Spanwise Control Stations.

2.1 Blade Optimization Variables

The NRT blade is an aerodynamic shell design with structural spar, using a single shear web centered on the spar caps for improved access to instrumentation. There is no leading edge or trailing edge reinforcement required or used due to the short 13 m blade length not being significantly affected by gravity loads. For the NRT structural blade optimization the following variables were chosen in the optimization with limits as described:

Spar Cap Width: Allowed to vary between $[100, 700]$ mm.

Root Build-up: Thickness at inner span location allowed to vary between $[10, 40]$ mm at variable span between $[0.05, 0.14]$; thickness at outer span location is $[1]$ mm at variable span between $[0.15, 0.19]$.

Spar Cap Thickness: Thickness at the beginning of the spar at 0.05 span location allowed to vary between $[1, 13]$ mm; inner thickness at 0.20 span location allowed to vary between $[1, 13]$ mm; inner thickness at 0.50 span location allowed to vary between $[1, 13]$ mm; thickness at the end of the spar at 0.95 span location allowed to vary between $[1, 13]$ mm.

The blade design optimizes these eight variables in accord with a fitness function. For the NRT blade the requirements drive the design differently than a standard blade design optimization. The blade requirement of nearing the blade weight and rotor inertia of the SWiFT OEM rotors sets a mass constraint to meet. Additionally, the requirement to have a "rigid" blade for ease of modeling and producing high-quality validation datasets results in a preference to increase blade stiffness, all else equal. These two constraints then define the fitness function for the NRT blade structural optimization which is to maximize frequency with a weight maximum equal to the SWiFT OEM blade. Penalties are added to the iteration score based on exceeding the SWiFT OEM mass, exceeding the maximum allowable tip deflection from DLC analysis, and if there is an edge-flap frequency ratio value below 1.3.

The remaining NRT blade station structural properties are defined in the optimization as follows:

Gelcoat: Thickness of 1 mm over the entire blade.

Inner and Outer Shell: Thickness of 2 mm over the entire blade.

Single Shear Web: Fiber thickness of 2 mm, core thickness of 10 mm, fiber thickness of 2 mm from 0.05-0.90 span.

Carrot Material: Used to add the 39 kg mass of the 30 carrots used for mounting the blade to the hub on the SWiFT turbine. Carrot mass adjusted density material thickness is 40 mm from 0-0.0154 span. Outer root material is used to space the carrots so that they are centered on the blade bolt circle and maintain the blade root diameter equal to the SWiFT OEM turbine.

Shell Panel Core: Thickness of 1 mm at 0.05 span, thickness of 15 mm at 0.20 span, thickness

of 10 mm at 0.50 span, thickness of 1 mm at 1.0 span.

The NRT blade components have material assignments from the materials listed in Table 2.1. The blade is an all-glass design using uni-axial glass (ELT-5500), bi-axial glass (EBX-2400) and tri-axial glass (ETLX-2400). Material assignments are as follows; shell material, bi-axial glass; spar material, uni-axial glass; root build-up, tri-axial glass; shear web, bi-axial glass; all core material used is foam with a 200 kg/m^3 density.

Table 2.1. NRT Blade Material Properties.

Material	E_x $[MPa]$	E_y $[MPa]$	G_{xy} $[MPa]$	Density $[kg/m^3]$
Gelcoat	3440	-	-	1235
ELT-5500	47835	18197	2826	1950
EBX-2400	17183	17183	9202	1900
ETLX-2400	20333	9305	4756	1900
Airex C70-200	175	175	75	200

2.2 Blade Optimization Result

The final optimization was run with a population size of 80 for 50 generations, using the described inputs. This population size was chosen from a sensitivity analysis, with the eight optimization variables, which revealed variance in final optimization runs with smaller population sizes and was chosen to be conservative. The current optimization solver utilized is a global optimization genetic algorithm scheme. The progress and completion of the optimization is shown in Figure 2.2, with the optimization progress tracked in the top left subfigure. The optimization is shown to converge around the thirtieth generation.

The structural blade was optimized to maximize frequency with a mass limit equal to the SWiFT OEM rotor mass. The optimization resulted in a blade with a 518 mm spar cap width and spar cap thickness and root build-up as shown in Figure 2.3. The optimized root build-up was within the limits set on the variables so these limits are determined to be sufficient. The optimized spar cap width is a constant along the blade until the blade station chord is too low to allow for this width of spar cap, at which point the spar cap width is scaled proportionately with the station chord. The root build-up shown in Figure 2.3(b) is a stacked graph showing the root carrot hardware location with supporting root-inner and root-outer tri-axial glass material. This was added to the model to represent the weight added by the 40 kg of root hardware and to more accurately represent the amount of surrounding material necessary to connect to the 40 mm diameter root carrots.

For the optimized blade, S0, the resulting overall properties are listed in Table 2.2. Maximizing the frequency with the variable design limits resulted in a 632 kg blade with a 3.2 p first flap frequency. It is interesting to note that the mass limit on the optimization was not reached. This means additional material that was allowed to be added to the blade increased the flap stiffness less

than the mass and therefore would only reduce the frequency, which was being maximized. A way to remove this effect is to allow the spar cap thickness to be greater than the 13 mm limit, which is undesired from a manufacturing perspective.

The properties listed in Table 2.2 can now be used to verify some of the requirements described in Section 1.1. The first flap frequency for the S0 blade, 3.2 p, is outside of the critical band around the blade pass frequency of 2.9-3.1 p. The edge-flap ratio for the S0 blade, 2.0, is greater than the required ratio of 1.3 ensuring the modes are not coupled. Blade mass and rotor inertia are desired to be near that of the OEM blade and the S0 blade has an inertia that is 12% lower than the OEM blade, from comparing simulation models. The difference in the mass between the model and measured values of the SWiFT OEM blade is due in part to the 40 kg of blade root hardware not being included in the model. This hardware does not significantly affect the rotor inertia, however, where only 10 $kg\ m^2$ would be added to the blade inertia.

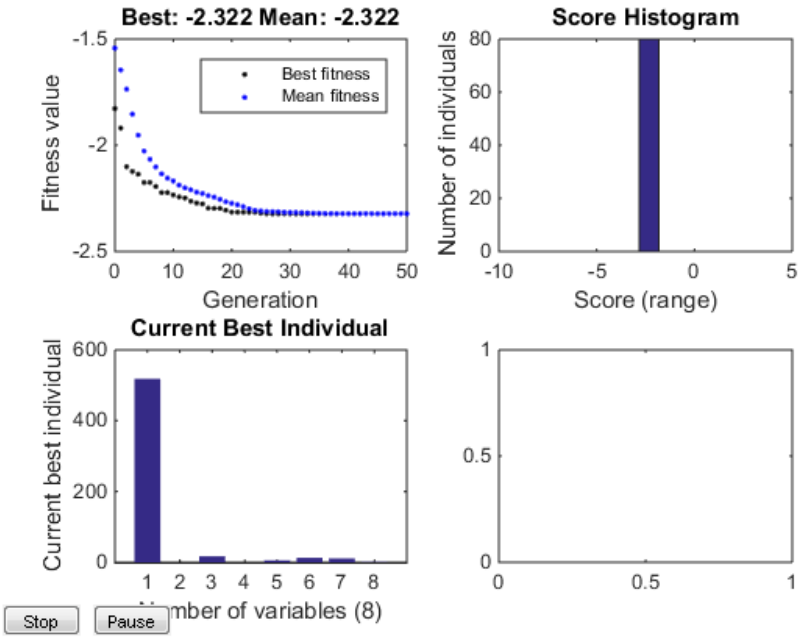

Figure 2.2. Structural Optimization Progress.

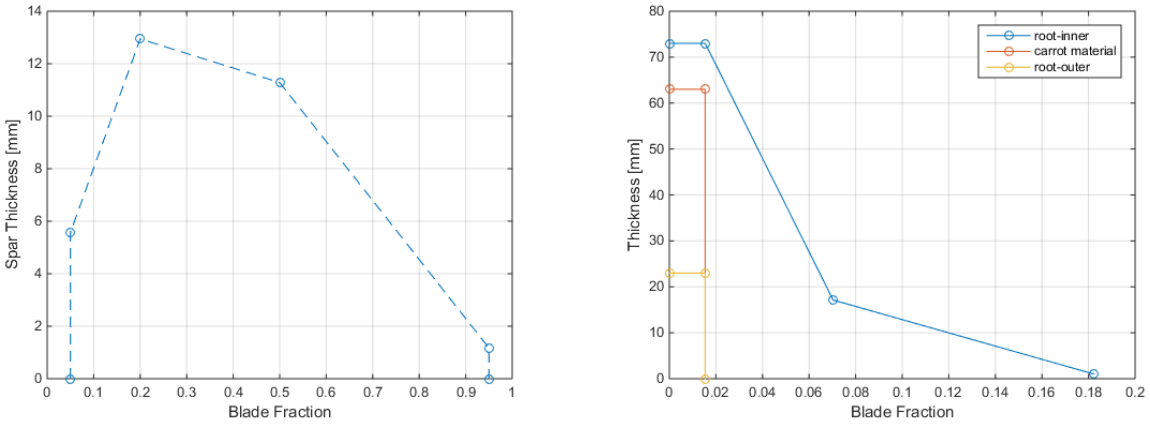

(a) Optimized Spar Thickness

(b) Optimized Root Build-up

Figure 2.3. Results of the Structural Optimization, Structural Design S0.

Table 2.2. Blade Optimization Results and OEM Comparison.

	NRT S0 - All-glass	SWiFT OEM Rotor (model)	SWiFT OEM Rotor (measured)
First Flap Frequency	2.32 hz (3.2p)	2.28 hz (3.2p)	2.34 hz (3.2p)
First Edge Frequency	4.74 hz (edg/flp = 2.0)	3.40 hz (edg/flp = 1.5)	3.81 hz (edg/flp = 1.6)
Weight	632 kg	597 kg	659 kg
Blade Inertia ($kg\ m^2$)	20,141	22,881	n/a

This page intentionally left blank.

Chapter 3

SWiFT Turbine Loads Analysis

The standard structural requirements placed on the NRT rotor are to ensure safe operation on the SWiFT turbines. This is verified by simulating the most pertinent IEC design load cases described in Section 1.1 and comparing them to known allowable loads or, in the absence of known allowable loads, to the SWiFT OEM Rotor loads. The confidence in comparing loads to the OEM machine comes from this machine having been in operation for twenty-plus years across the globe in many high wind sites as proof of the machine's robustness. For this class III-C site it is deemed sufficient to stay beneath the loads of the OEM machine where actual component allowable loads are not known with acceptable certainty.

Table 3.1 summarizes the results for the NRT S0 rotor and the SWiFT OEM rotor for several pertinent loads. These loads are in categories of blade loads which describe the safety of the blade, tower loads which describe the safety of the yaw system and foundation, and low speed shaft loads which are used to determine the reliability of the low speed shaft bearing in fatigue. In each of the categories the design strength and design loads are compared, as defined in Equation 3.1.

$$F_d = \gamma_F F_k \tag{3.1}$$

The design load, F_d, is the characteristic load, F_k, multiplied with the partial safety factor, γ_F, as prescribed in the standard. In Table 1.2 the partial safety factor for each of the DLC's simulated is for a "normal" design situation which prescribes a $\gamma_F = 1.35$. In Table 3.1 the design strength and loads are compared with this safety factor used to convert the simulation characteristic loads into design loads in all cases. The one exception to this is for the blade tip deflection, where a critical displacement safety factor, γ_d, is used as described in Equation 3.2. This safety factor includes uncertainty due to the load calculation, $\gamma_F = 1.35$, material properties, $\gamma_m = 1.1$, and consequences of failure, $\gamma_n = 1.0$, and results in a value of $\gamma_d = 1.485$ for the critical displacement safety factor which is multiplied onto the characteristic displacements from the DLC analyses.

$$\gamma_d = \gamma_F \gamma_m \gamma_n \tag{3.2}$$

The resulting design loads for the NRT S0 rotor and SWiFT OEM rotor are compared in Table 3.1. Comparing the NRT blade loads to the respective allowable strength satisfies the requirements related to blade survivability and maximum out of plane tip deflection. As an additional verification, these loads and deflection are less than the SWiFT OEM design. In all compared load cases

the magnitude of the NRT rotor loads are lower than the SWiFT OEM loads. This gives confidence in the SWiFT machine survivability when deploying the NRT rotor, notably for yaw and drivetrain components. The loads caused by the tower base moments are also well within the foundation limits.

Table 3.1. NRT Rotor Loads Comparison.

Load Direction	Allowable Loads	NRT Rotor Design Loads	SWiFT Rotor Design Loads
		Blade Loads	
Root Edge Bending	(-210,210) kNm	(-37.8, 67.9) kNm (DLC 1.3 ETM; 21 m/s / 15 m/s)	(-60.1, 83.8) kNm (DLC 1.3 ETM; 23 m/s / 13 m/s)
Root Flap Bending	(-210,210) kNm	(-119.7, 177.1) kNm (DLC 6.1 EWM50; -15 deg / +15 deg)	(-141.3, 181.7) kNm (DLC 6.1 EWM50; -10 deg / +15 deg)
Blade Tip Deflection	1.97 m	0.68 m (DLC 1.3 ETM, 19 m/s)	0.97 m (DLC 1.3 ETM, 15 m/s)
		Tower Loads	
Nacelle Yaw Moment	n/a	(-93.7, 82.2) kNm (DLC 1.3 ETM, 23 m/s, 11 m/s)	(-132.6, 101.0) kNm (DLC 1.3 ETM, 21 m/s / 23 m/s)
Tower Base Overturning	4510 kNm	(-952.0, 988.4) kNm (DLC 6.1 EWM50, -15 deg / +15 deg)	(-892.5, 1388.3) kNm (DLC 6.1 EWM50, -15 deg / 15 deg)
Tower Base Overturning	4510 kNm	(-573.0, 1191.3) kNm (DLC 1.3 ETM, 5 m/s / 15 m/s	(-950.5, 1716.1) kNm (DLC 1.3 ETM, 5 m/s / 19 m/s)
		Low Speed Shaft Bearings	
LSS Inline Force	n/a	46.0 kN (DLC 1.3 ETM, 17 m/s)	52.7 kN (DLC 1.3 ETM, 15 m/s)
LSS tip horizontal shear	n/a	(-39.4, 30.1) kN (DLC 6.1 EWM50, +15 deg / -15 deg)	(-44, 27.4) kN (DLC 6.1 EWM50, +15 deg / -15 deg)
LSS tip vertical shear	n/a	(-46.7, -28.8) kN (DLC 1.3 ETM, 23 m/s / DLC 6.1 EWM50, -15 deg)	(-50.5, -25.4) kN (DLC 1.3 ETM, 23 m/s)
LSS Torque	n/a	(-24.2, 98.4) kNm (DLC 6.1 EWM50, 0 deg / DLC 6.3 EWM1, -30 deg)	(-138, 111.6) kNm (DLC 6.1 EWM50, 0 deg / DLC 1.3 ETM, 23 m/s)
LSS tip non-torque, horizontal	n/a	(-76.1, 102.5) kNm (DLC 1.3 ETM, 19 m/s / 21 m/s)	(-100.4, 137.2) kNm (DLC 1.4 ECD, V_r+2 / DLC 1.3 ETM, 21 m/s)
LSS tip non-torque, vertical	n/a	(-91.8, 85.5) kNm (DLC 1.3 ETM, 23 m/s / 11 m/s)	(-133.5, 113.5) kNm (DLC 1.3 ETM, 21 m/s / 23 m/s)

Chapter 4

Additional Blade Requirements

Additional requirements are placed on the NRT blade beyond turbine survivability. These requirements are derived from the main objective of the NRT rotor which is to provide high-quality validation datasets. These additional requirements are to ensure model predictability by reducing uncertainty in the blade aerodynamic performance due to aeroelasticity and enable accurate modeling of the NRT rotor as a "rigid" blade set.

4.1 Additional Requirements Description

The requirements placed on the blade to ensure modeling objectives are met are as follows:

Sufficient Flap Stiffness: The blade shall have sufficient flap stiffness such that section body velocities do not induce dynamic changes in section angles of attack which vary more than 1 degree from nominal, steady design values for Region II operation.

Sufficient Torsional Stiffness: The blade shall have sufficient torsional stiffness such that the blade sections do not experience dynamic changes in section angles of attack which vary more than 1 degree from nominal, steady design values for Region II operation. Effects on pitch moment due to section C_m and blade sweep shall both be considered.

No Twist Coupling: The blade structure shall be designed such that there is minimal coupling of twist deflection with any other blade elastic degrees of freedom.

Structural Linearity: The blade tip shall not deflect more than 5% of blade length under any normal operating loads. A blade structure which does not deflect more than 5% of its length is assumed to have linear elastic behavior.

Design for Loaded Operation (static twist): Static blade twist distribution shall be designed to match a target distribution at a single operating point of $U_\infty = 6\ m/s$ (a middle wind speed in Region II). Deviation from nominal twist design at other operating points in Region II shall not exceed 0.5 deg. This requirement is meant to ensure that the blade performs as intended under steady aeroelastic loading at the stated operating wind inflow speed.

4.2 Aeroelastic Analysis of the NRT Rotor

Aeroelastic simulations of the NRT S0 rotor were performed to ensure satisfaction of the additional requirements added to ensure model predictability of the rotor. These simulations are performed using FAST with the optimized structural blade properties and aerodynamic design described by Kelley [2]. The additional requirements are placed on Region II operation and tested in unsteady conditions using TurbSim to generate both IEC class C (low) and A (high) turbulence. Region II for the NRT rotor operating on the SWiFT machine is defined between 3-6.9 m/s and tested at top and bottom of Region II using 4 and 6 m/s averages. These turbulence classes correspond to turbulence intensities (TI) of 25% and 35% at 4 m/s, and 18% and 25% at 6 m/s. Even with the "low" class C turbulence, the turbulence intensity is significantly higher than the average at the site, as seen in Figure 1.1. This gives confidence in the sufficiency of the comparison to follow as reduced fluctuations in the velocity would reduce the aeroelastic dynamic effects and uncertainty. Additionally, a limit on TI can be added to the experimental campaigns, which is easily obtainable at the site, to further reduce the aeroelastic effects if desired.

4.2.1 Angle of Attack Change due to Bending

The first check is that there is sufficient flap stiffness such that body velocities do not induce dynamic changes in section angle of attack greater than 1 deg. The first check is to compare the effect of elasticity in the flap and edge directions to a true rigid blade model. This is performed in FAST by comparing the S0 elastic blade model with a model where the blade degrees of freedom are turned off making it truly rigid. An additional source of uncertainty which adds to angle of attack variation from anticipated 2-d performance is the Beddoes-Leishman dynamic stall model. This model's contribution was compared as well in the initial analysis with FAST. Figure 4.1 shows simulation results comparing the rigid blade with no stall model with the elastic blade results without and with use of the stall model. The rigid blade without stall model serves as the result with the least variance on angle of attack and is used as the best case scenario for variance of angle of attack. The results shown are for 6 m/s, class C turbulence operation at four span stations. For the three simulations a 10 sec moving average is shown with one standard deviation error bars. The important thing to compare here is not the size of the error bar, but that size relative to the benchmark rigid blade without stall model. The absolute size of the error bars is additionally influenced by the turbulence.

From the Figure 4.1 results you can see that the difference in angle of attack and its variance due to elasticity, and even the difference due to elasticity plus the stall model are nearly indistinguishable and in all cases less than 0.5 deg. Over the outer 50% of the blade the difference in these Region II FAST simulations of angle of attack is nearly absent. The conclusion from these results is that the 13 m NRT S0 blade, with a stiffness resulting in a 3.2 p first flap frequency, will have negligible influence on the angle of attack variation due to blade station body velocities. The variance in angle of attack purely due to turbulence, shown with the rigid blade without stall model simulation, is much greater than the added variance caused by body velocities due to elasticity which is nearly negligible in this comparison.

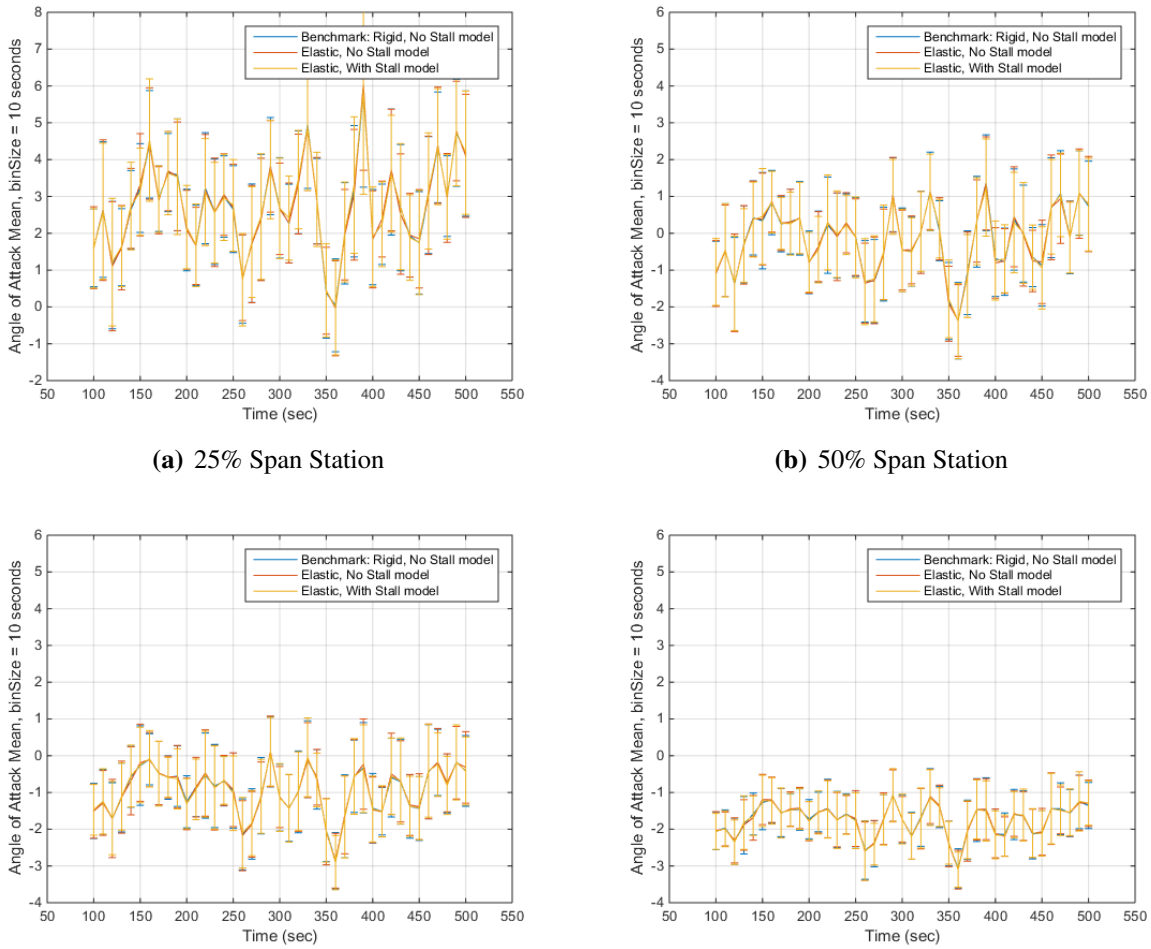

(a) 25% Span Station

(b) 50% Span Station

(c) 75% Span Station

(d) 95% Span Station

Figure 4.1. FAST Angle of Attack Variation in Turbulence with Elasticity, 6 m/s, IEC Class C.

In order to verify these results, an analytical check is performed using the FAST output to then calculate the angle of attack directly, in order to compare to the FAST angle of attack calculation. The velocity diagram for a wind turbine airfoil station with included body velocities is shown in Figure 4.2. Rotor induction factors arising from the induced velocity, w, which is perpindicular to the relative velocity, W_{rel}, adds to the rotational velocity and subtracts from the axial velocity. The body velocities due to elasticity, V_e, are included in the diagram for both the in plane and out of plane components. The body velocities affect both the angle of attack and the magnitude of the relative velocity. There is a distinction in how the effect of body velocities are included, based on whether they affect the induction or not. If the body velocities are considered to affect the induction the angle of attack is calculated using Equation 4.1. If the body velocities are assumed to not affect induction, then they can be added into the velocity triangle after the effect of induction is included, as in Equation 4.2. This results in four possible combinations for how to include the effect of body

velocities. Equation 4.2 was ultimately chosen to describe the angle of attack because it results in the largest influence from the out of plane body velocity and serves as more of a worst case scenario.

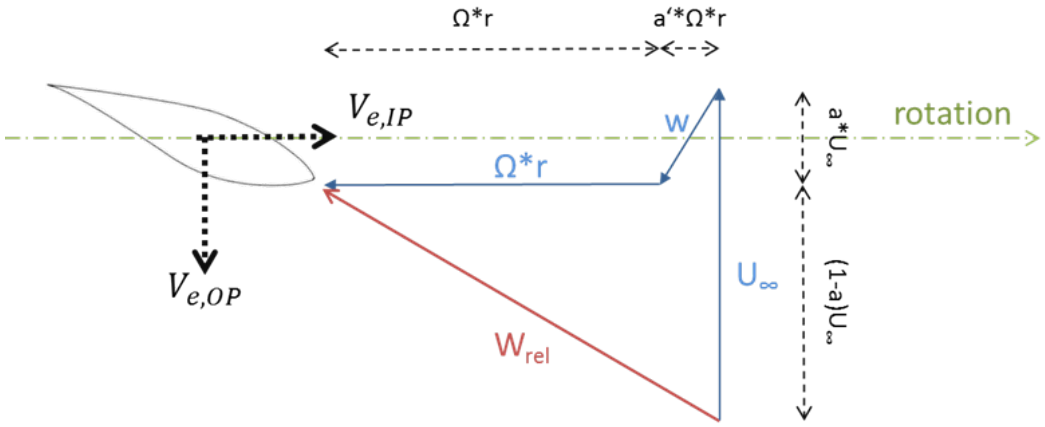

Figure 4.2. Wind Turbine Velocity Triangle with Body Velocities.

$$tan(\alpha+\beta)=\frac{(U_\infty+V_{e,OP})(1-a)}{(\Omega r+V_{e,IP})(1+a')} \tag{4.1}$$

$$tan(\alpha+\beta)=\frac{U_\infty(1-a)+V_{e,OP}}{\Omega r(1+a')+V_{e,IP}} \tag{4.2}$$

Equation 4.2 is solved for the angle of attack, α, in terms of the body velocities, induction factors, operational tip speed ratio and blade set angle at each blade station, Equation 4.3.

$$\alpha=tan^{-1}\left[\frac{1}{TSR\frac{r}{R}}\frac{1-a+\frac{V_{e,OP}}{U_\infty}}{1+a'+\frac{V_{e,IP}}{\Omega r}}\right]-\beta \tag{4.3}$$

To verify the FAST results in Figure 4.1, Equation 4.3 is used with FAST outputs for each of the terms on the right hand side of the equation. This angle of attack calculation is then compared to the FAST results as a rough-order verification of the FAST results. The angle of attack (AoA) comparison is shown in Figure 4.3 for four span stations. Body velocities are calculated using the time history of the simulation results for tip deflections. Span station body velocities are calculated by assuming a linear deflection from root to tip. This is again a worst case scenario for the inner span stations, and is a safe assumption.

The calculated values do not include the time history of angle of attack effects, so they are not considered to be accurate in the average. The comparison to be made here is of the variance in angle of attack by comparing error bar lengths. FAST simulation angle of attack results for the NRT S0 blade are compared with calculated angle of attack using Equation 4.3 when both including body velocities and not. Two comparisons can be made with conclusions drawn. By comparing the FAST AoA with the calculated AoA with body velocities it is observed that the variance of AoA in the FAST results are on the same order of magnitude as those calculated analytically, comparing the blue and yellow curve error bar lengths. In most cases, the variance in AoA shown in the FAST results are greater than those for the calculation of AoA with body velocities. This gives additional confidence in the FAST results. The second comparison to be made, which is a more direct comparison, is between the calculated AoA results when including body velocities and when not. At each span station you can see that the calculation including body velocities has only slightly higher variance than the calculation without body velocities, revealing less than 0.25 deg increase in the variance of AoA due to elasticity of the S0 blade. This second analysis also reveals no significant uncertainty added to AoA with S0 blade.

A final check on the effect of bending stiffness on dynamic angle of attack variation is performed to further verify the satisfaction of the S0 blade on meeting the flap stiffness requirements. This is done now completely analytically using Equation 4.2 to determine the effect of body velocities on the angle of attack. A contour line plot of the angle of attack change due to in plane and out of plane body velocities is shown for the four span locations in Figure 4.4. These plots assume that the variables in the right hand side of Equation 4.3 are all constant other than the body velocities. This assumption means that the turbine controller holds the turbine to a perfectly constant TSR, and that rotor induction does not change with changing wind speed or body velocities. From these figures the effect of the same magnitude body velocity is seen to be more significant as you move inboard. This is due to the reduced rotational velocity inboard which dominates the AoA calculation as you move outboard. Conversely, the body velocities are smaller inboard due to the reduced length from the fixed end and the higher stiffness.

Body velocity histograms of the simulation results in turbulent operation are shown for the S0 blade in Figure 4.5 at the same four span stations, shown non-dimensionally. The out of plane body velocity is around two orders of magnitude greater than the in plane body velocity due to the increased stiffness in plane and the higher outboard station rotational velocity than axial velocity. The values from Figure 4.5 can be added into Figure 4.4 to determine the AoA variation due to body velocities, given the mentioned constraints and assumptions. This comparison is performed and shown in Table 4.1 showing the 2σ, 95% confidence interval of the blade station body velocities and the resulting AoA variation from the statically deflected value. This analysis shows a maximum AoA variation of ± 0.88 deg for 95% of the time history, which is within the 1 deg bending limit set by the requirement.

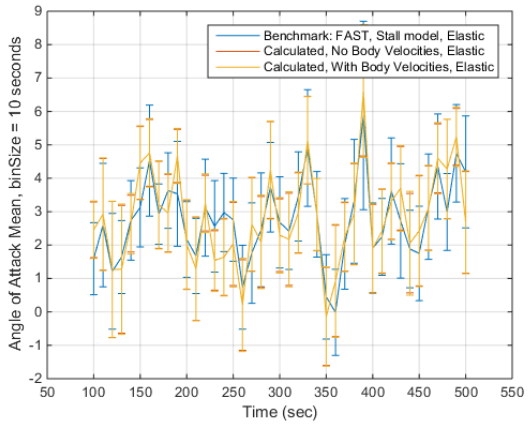

(a) 25% Span Station

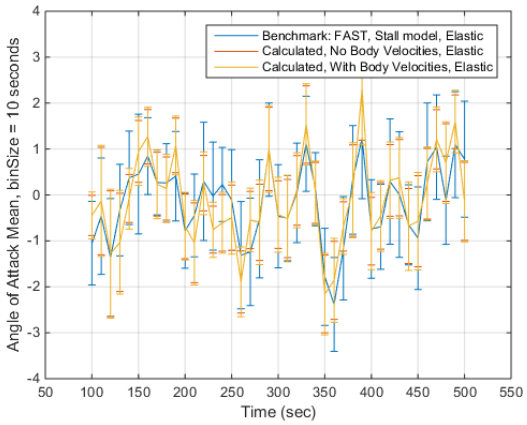

(b) 50% Span Station

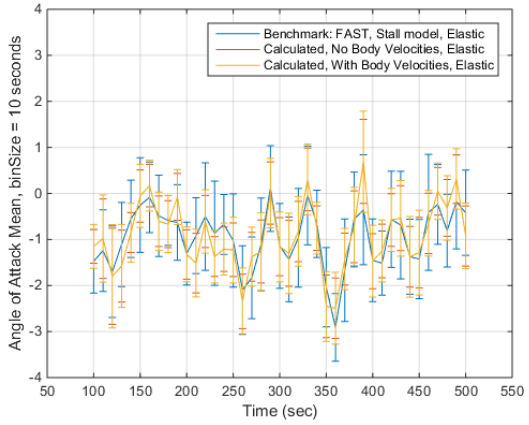

(c) 75% Span Station

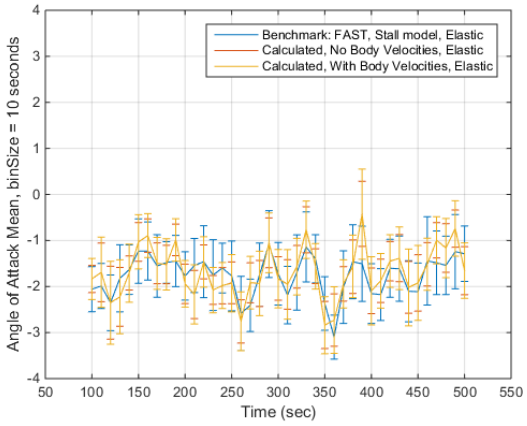

(d) 95% Span Station

Figure 4.3. Calculated Angle of Attack Variation in Turbulence, 6 m/s, IEC Class C.

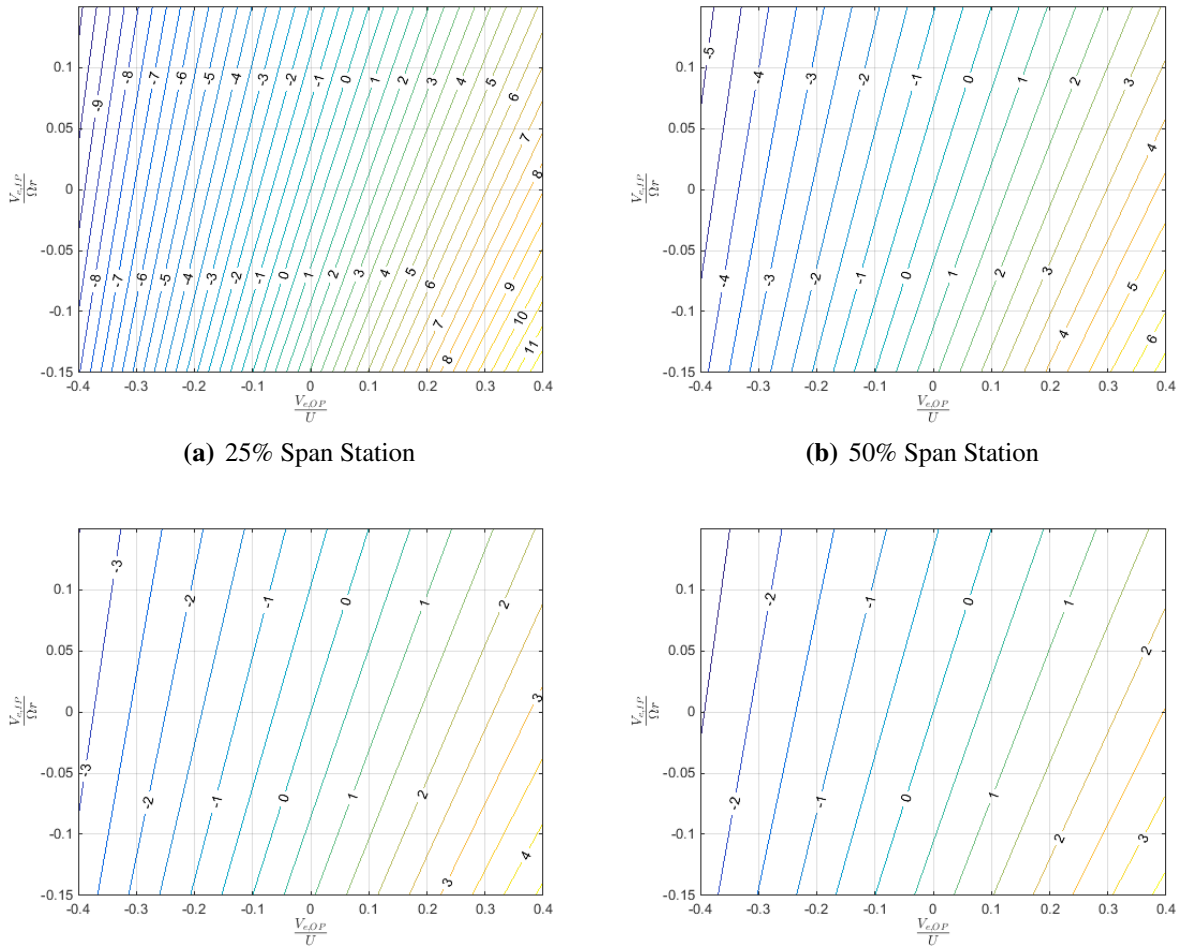

(a) 25% Span Station

(b) 50% Span Station

(c) 75% Span Station

(d) 95% Span Station

Figure 4.4. Calculated Angle of Attack Variation due to Body Velocities.

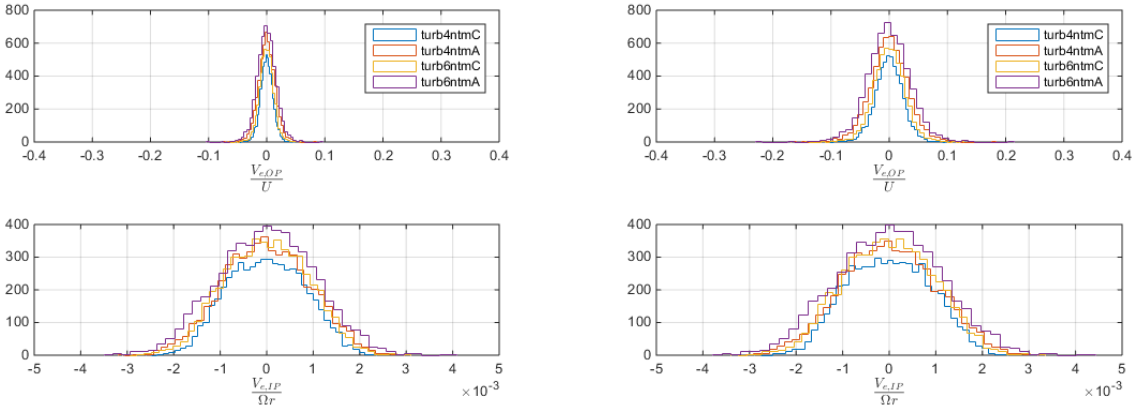

(a) 25% Span Station

(b) 50% Span Station

(c) 75% Span Station

(d) 95% Span Station

Figure 4.5. FAST Calculation of Non-Dimensional Body Velocities.

Table 4.1. Non-dimensional Body Velocities and Their Effect on Angle of Attack.

Non-dimensional Out of Plane Body Velocity, 95% Probability

Span Location	4 m/s, class C	4 m/s, class A	6 m/s, class C	6 m/s, class A
25%	0.0210	0.0294	0.0240	0.0326
50%	0.0462	0.0646	0.0530	0.0718
75%	0.0688	0.0962	0.0790	0.107
95%	0.0884	0.124	0.101	0.137

Non-dimensional In Plane Body Velocity, 95% Probability

Span Location	4 m/s, class C	4 m/s, class A	6 m/s, class C	6 m/s, class A
25%	1.62e-3	1.84e-3	1.77e-3	2.06e-3
50%	1.76e-3	2.00e-3	1.93e-3	2.24e-3
75%	1.80e-3	2.04e-3	1.97e-3	2.28e-3
95%	1.82e-3	2.08e-3	1.99e-3	2.32e-3

Body Velocity Effect on Angle of Attack, $\Delta\alpha$ (deg), 95% Probability

Span Location	4 m/s, class C	4 m/s, class A	6 m/s, class C	6 m/s, class A
25%	0.49	0.68	0.57	0.76
50%	0.56	0.78	0.65	0.87
75%	0.56	0.78	0.65	0.87
95%	0.57	0.80	0.65	0.88

4.2.2 Angle of Attack Change due to Torsion

The second check on the blade to ensure modeling accuracy is on the torsional stiffness and the effect of torsional elasticity on the angle of attack. The requirement is to ensure that dynamic AoA variation does not exceed 1 deg in Region II. FAST does not currently have a torsional degree of freedom and therefore the effect of torsional deflection is not accounted for in the angle of attack. The blade model from NuMAD does however model the torsional rigidity of the blade so it is possible to calculate the twist due to torsion from the FAST output forces and moments and the blade model station torsional properties. This calculation is performed as the check for satisfaction of the torsional stiffness requirements for the S0 blade, following Equation 4.4. This calculation is performed from root to hub by determining the elemental twist from the summation of all outboard moments and forces. The net torsion at each element is a sum of the pitch moment and elemental forces multiplied with respective out of plane and in plane moment arms from sweep and prebend, with blade deflection, Equation 4.5. The twist is then added to all inboard elemental twist deflections to get the station twist, as shown in Equation 4.6.

$$d\theta_i = \left(\frac{l}{GJ}\right)_{element} \Sigma_{n=i}^{N} T_{n,PitchAxis} \tag{4.4}$$

$$T_{n,PitchAxis} = M_{p,n} + (Lcos\phi + Dsin\phi)_n(s + d_{IP})_n + (Lsin\phi - Dcos\phi)_n(p + d_{OP})_n \tag{4.5}$$

$$\theta_i = \Sigma_{n=1}^{i} d\theta_n \tag{4.6}$$

This analysis procedure was used with the results for the four wind speed/turbulence class simulations to analyze the maximum blade deflection due to torsion at the blade tip for the S0 blade. The time history of tip twist from the 10 min turbulent wind files are shown in Figure 4.6. To determine the dynamic change in angle of attack at the tip, a moving average was performed on the dataset with a 90 sec window. The 90 sec window was chosen as it corresponds to the time required at 4 m/s wind speed for the wake to advect downstream the largest turbine-turbine spacing at SWiFT, 6 rotor diameters, and for 20 rev to average the data over. At 6 m/s, this time corresponds to an averaging time of 40 rev with 6 D wake advection.

The figure shows this moving average of the maximum twist due to torsion with ± 2 standard deviations, corresponding to the 95% probability. This 95% probability is the dynamic change in angle of attack and is plotted alone in the lower subplot for each wind class, and should be compared against the 1 deg maximum twist deflection requirement. One thing to be noted from the time series is that the 2 standard deviation dashed lines are nearly always greater than the bounds of the time series. This is due to assuming a normal distribution to calculate the standard deviation which from observation is clearly not a valid assumption over much of the time history due to the lower frequency variation in twist. This error in calculating the variance of tip twist adds a safety factor onto the results and the results are then a worst case scenario.

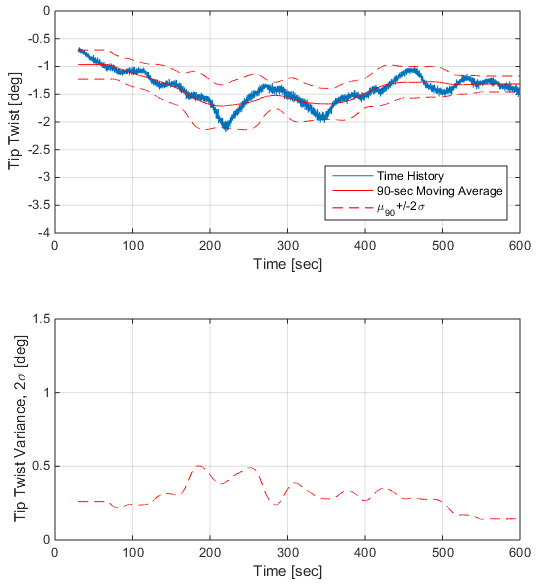

(a) 4 m/s, Class C Turbulence

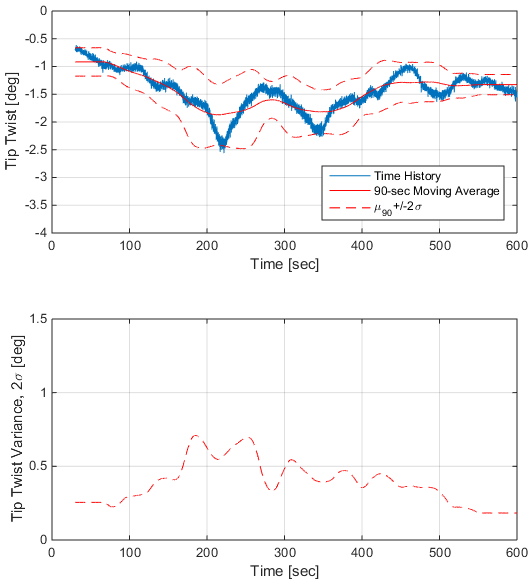

(b) 4 m/s, Class A Turbulence

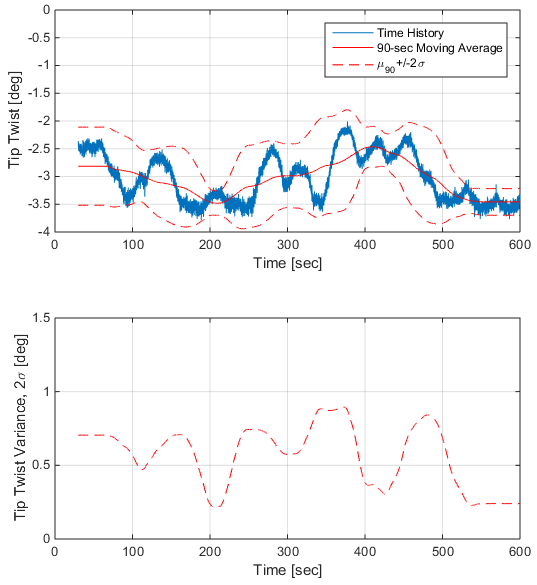

(c) 6 m/s, Class C Turbulence

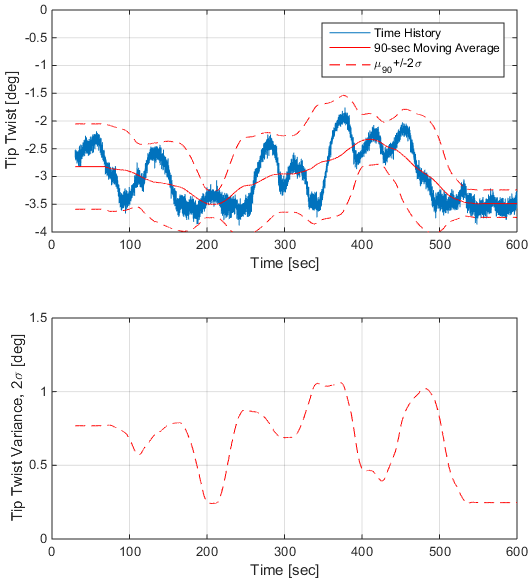

(d) 6 m/s, Class A Turbulence

Figure 4.6. Blade Tip Twist in Turbulent Operation.

The analysis shown in Figure 4.6 reveals maximum dynamic twist change in AoA of less than 1 deg for all but the 6 m/s, class A turbulence simulation where results are slightly higher than 1 deg, but due to the data in this window not having a normal distribution. Additionally, this wind class corresponds to a turbulence intensity of 25% which is high and the experimental campaign could filter out datasets with a TI exceeding a lower value, if desired. The conclusion then is that the S0 blade has sufficient torsional stiffness to meet the dynamic angle of attack variation due to torsion requirement.

4.2.3 Blade Static Deflections

The final requirements to check for the S0 blade that relate to model predictability within Region II operation are to ensure the structural linearity assumption for the blade and to determine the uncertainty to which the blade can be designed for loaded operation. The structural linearity requirement is set that the blade not deflect in a bending mode greater than 5% of the 13 m blade length, which is 0.65 m. Figure 4.7 shows the deflection histogram for out of plane and in plane bending for turbulent operation within Region II. The in plane deflection is an order of ten smaller than for out of plane, so the comparison will be for out of plane alone. The plot reveals that maximum deflection is less than 0.25 m in even the high class A turbulence which satisfies the response and means there is less than 2% deflection in Region II.

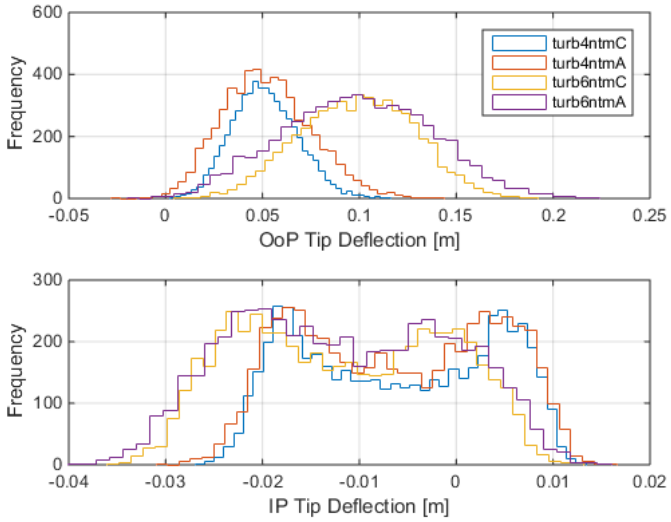

Figure 4.7. Blade Tip Deflection in Turbulent Operation, Design S0.

The design for loaded constraint on static twist is defined as designing the blade for a 6 m/s wind speed and that there is not greater than 0.5 deg variation from this twist within Region II. Figure 4.8 shows the amount of twist at the tip of the blade for steady operation, and the red dashed

box defines Region II for the NRT rotor. To meet the 0.5 deg requirement of maximum twist at the tip would mean that the turbine could only operate between approximately 5 and 7 m/s, with the torsional stiffness of the S0 blade. The blade torsional stiffness decreases as you move outboard due to the smaller thickness and chord meaning the amount of twist is not a linear relationship with blade span. Figure 4.9 shows the amount of twist at distinct spanwise stations, focusing on Region II operation from 3-6.9 m/s. A bound can then be made where the change in angle of attack due static twist is less than 0.5 deg in Region II on percent of span. The 60% blade span location has a total twist of around 1 deg meaning it is possible to have a ± 0.5 *deg* static twist variance. The S0 blade then does not meet the static twist requirement outboard of 60% blade span.

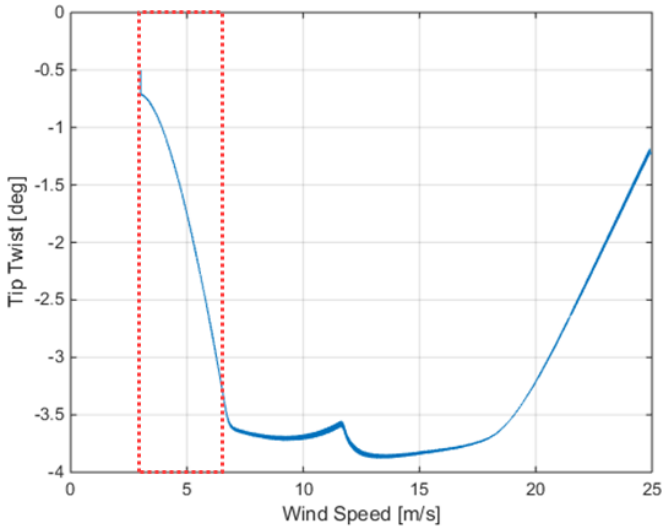

Figure 4.8. Static Tip Twist in Steady Operation, Design S0.

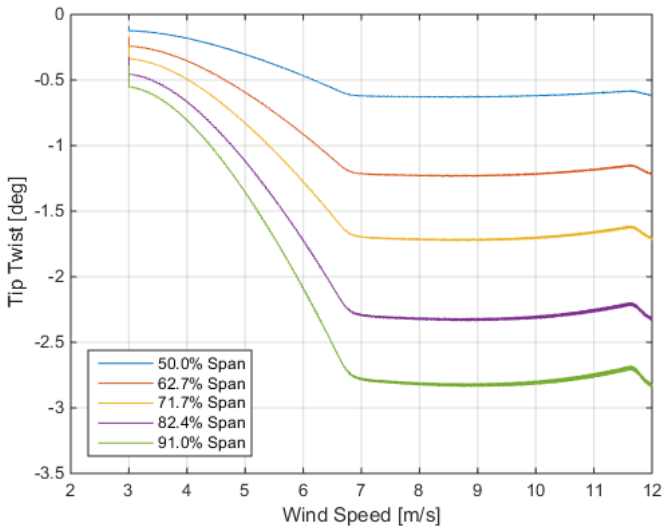

Figure 4.9. Static Twist at Spanwise Stations in Steady Operation, Design S0.

Conclusion

A structural design has been produced for the first National Rotor Testbed blade series. The blade structural optimization of maximizing frequency with the constraint to not exceed the SWiFT OEM blade weight resulted in a 632 kg blade with a 3.2 p first flap frequency. Requirements for NRT blade and SWiFT turbine survivability were tested and ensured through simulation. Comparison of the NRT rotor was made to machine allowable loads, where known, or alternatively to SWiFT OEM rotor loads. **In all tested design load cases the NRT rotor was below the allowable loads and the SWiFT OEM loads, which allows for safe operation of the NRT rotor at SWiFT**.

The goal of the S0 blade series is to remove some of the realistic behavior of modern-day utility wind turbines to reduce modeling uncertainty for model validation. The result is a "rigid" blade requirement to remove the effects of aeroelasticity to an acceptable degree and satisfy simplifying model assumptions. The defining question was addressed of how rigid is rigid enough? Strict requirements are placed on the aeroelastic performance of the NRT S0 blade to have less than ± 1 deg dynamic change of angle of attack caused by both bending and torsion which were tested through simulation.

Three methods of analysis were tested to verify that body velocities caused by bending deflections do not cause greater than 1 deg variation in the angle of attack. **Each method reveals less variation in Region II than the requirement allows ensuring that model uncertainty due to flap stiffness will be acceptably low for the S0 blade**. Torsional stiffness was tested using the results from simulation to calculate the torsional deflection of the blade. **Dynamic variation in angle of attack due to torsional elasticity stayed within the ± 1 deg requirement for all wind inputs except for the 6 m/s class C turbulence case, where the change in angle of attack extended just beyond 1 deg**. This was likely due to an incorrect method for calculating the standard deviation where a normal distribution is assumed. Additionally, were this case a concern, future experimental campaigns can mitigate the uncertainty by setting a limit on the maximum allowable turbulence intensity for validation data and choosing a value below the 25% TI for the 6 m/s, class C case.

Structural linearity of the S0 blade in Region II is satisfied where there is less than 2% deflection in flap bending. One requirement was not met by the S0 structural design, which is the design for loaded condition to design for static loading of the blade twist and for that to not deviate beyond ± 0.5 deg within Region II. **Outboard of 60% span the S0 blade does not satisfy the static twist requirement**. To ensure this requirement is met additional layers of cross-axis glass fabric can be added to the shell to increase the blade torsional stiffness until the range of static twist at the tip is reduced to meet the requirement. This requirement will be analyzed further, and modified or satisfied using the described method as best determined in the detailed design process. The S0 blade is suggested for pairing with the NRT aerodynamic design as a preliminary design which satisfies all of the requirements placed on it in accordance with the objective of the NRT

rotor, with exception of the static torsional deflection requirement but which can be met by adding torsional stiffness through the shell.

References

[1] *IEC 61400-1 Ed.3: Wind turbines - Part 1: Design Requirements*, 2005.

[2] Kelley, C. L., "Aerodynamic Design of the National Rotor Testbed," Tech. Rep. SAND2015-8989, Sandia National Laboratories, 2015.

[3] Resor, B. R., "National Rotor Testbed Requirements," Tech. Rep. SAND2015-9142, Sandia National Laboratories, 2015.

DISTRIBUTION:

1 MS 0899 Technical Library, 9536 (electronic copy)

Sandia National Laboratories